

Advancing Inorganic Coordination Chemistry by Spectroscopy of Isolated Molecules: Methods and Applications

Gereon Niedner-Schatteburg*^[a] and Manfred M. Kappes*^[b]

Abstract: A unique feature of the work carried out in the Collaborative Research Center 3MET continues to be its emphasis on innovative, advanced experimental methods which hyphenate mass-selection with further analytical tools such as laser spectroscopy for the study of *isolated* molecular ions. This allows to probe the intrinsic properties of the species of interest free of perturbing solvent or matrix effects. This review explains these methods and uses examples from

past and ongoing 3MET studies of specific classes of multicenter metal complexes to illustrate how coordination chemistry can be advanced by applying them. As a corollary, we will show how the challenges involved in providing well-defined, for example monoisomeric, samples of the molecular ions have helped to further improve the methods themselves thus also making them applicable to many other areas of chemistry.

Introduction

The synthetic chemistry of single center transition metal (TM) coordination compounds is well-established, not least because of the well-developed experimental arsenal of routine spectroscopic characterization methods commonly used in many chemistry departments worldwide. More recently quantum chemistry has become – almost – equally successful at modelling and predicting the properties of single center TM coordination compounds. The corresponding mutual bidirectional exchange of findings and ideas between theory and experiment (comprising both synthesis and characterization) is presently very fertile and drives ongoing success and applications in this area.

By contrast, the interaction of two, three or more nearby TM centers, when held in proximity within an oligonuclear compound, raises new questions resulting from the corresponding symmetry reduction and additional electronic couplings. For example, nominally closed shell metal centers may manifest attractive metallophilic interactions which give rise to proper-

ties showing a cooperative dependence on composition, separation and relative orientation of the TM centers. This is the realm of the DFG-funded Collaborative Research Center (CRC) TRR88 “Cooperative Effects in Homo- and Heterometallic Complexes (3MET)” which continues to pool corresponding research from TU Kaiserslautern and KIT – see editorial at the beginning of this issue.

Over the last ten years the development and application of novel experimental methods to probe structure and properties of *isolated* oligonuclear TM compounds has proven to be quite fruitful to extend our knowledge concerning this substance class – in an iterative, bidirectional feedback loop together with theory and synthesis (Scheme 1). Increasingly, benchmark experiments on isolated multicenter TM complexes empowers the long-term perspective of *in silico* design of selected optical, magnetic and catalytic properties based on the homo- and heterometallic complexes developed in 3MET.


For now, experiments on isolated molecular ions under well-defined conditions continue to be powerful for mapping and understanding the intrinsic properties of multicenter TM complexes because:

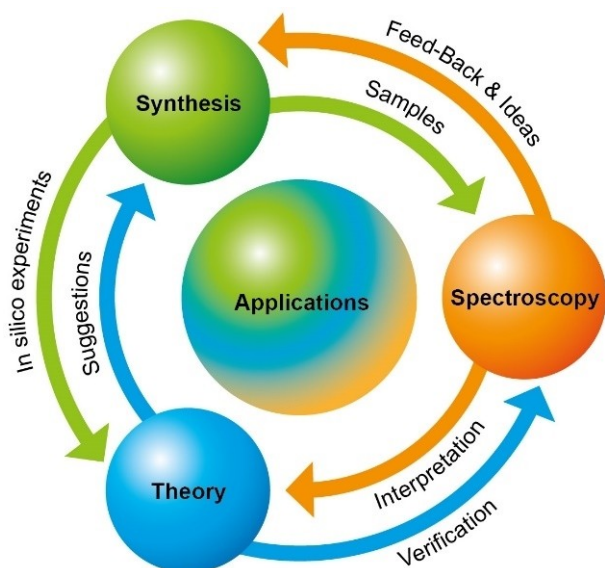
- (1) They allow verification and stimulate further development of theoretical methods for the description of the same species as accessed in the measurement;
- (2) In many cases permutative exchange of metal atoms in multimetal TM complexes can be achieved simply by selection of the desired mass-to-charge ratio from a mixture (otherwise requiring prohibitive condensed phase separation efforts); related experiments have turned out to be useful for probing differential many-body cooperativity.^[1]
- (3) Often the charge/redox state of the metal centers can be changed quantitatively (e.g. by varying electrospray ionization conditions) thus allowing to cleanly map their chemical and physical properties – whereas solution measurements typically integrate over mixtures;

[a] Prof. Dr. G. Niedner-Schatteburg
 Fachbereich Chemie and State Research Center OPTIMAS
 TU Kaiserslautern (TUK)
 67661 Kaiserslautern (Germany)
 E-mail: gns@chemie.uni-kl.de

[b] Prof. Dr. M. M. Kappes
 Institute of Physical Chemistry and Institute of Nanotechnology
 Karlsruhe Institute of Technology (KIT)
 76128 Karlsruhe (Germany)
 E-mail: manfred.kappes@kit.edu

 This manuscript is part of a Special Issue “Cooperative effects in heterometallic complexes”.

 © 2021 The Authors. Chemistry - A European Journal published by Wiley-VCH GmbH. This is an open access article under the terms of the Creative Commons Attribution Non-Commercial License, which permits use, distribution and reproduction in any medium, provided the original work is properly cited and is not used for commercial purposes.



Scheme 1. In the past, bi-directional interplay of synthesis and spectroscopy has driven the development of single center transition metal (TM) coordination chemistry. More recent advances in spectroscopic and computational methodologies have made possible the illustrated threefold synergetic approach which is considerably boosting our understanding of oligonuclear TM compounds. This review describes several of the corresponding advances in spectroscopic methodologies as related to studies of charged 3MET complexes in gas-phase.

Gereon Niedner-Schatteburg studied physics in Göttingen and graduated on crossed-beam scattering with Peter Toennies in 1988, did a postdoctoral stay with Y. T. Lee at UC Berkeley, and joined the group of Vladimir Bondybey at TU Munich working on kinetics of metal and molecular clusters. In 2000, he became chair of Physical Chemistry at TU Kaiserslautern where he conducts kinetic and spectroscopic studies of transition metal aggregates and clusters. He co-initiated and conducts the 3MET.de consortium with MMK in 2009.



Manfred Kappes studied chemistry in Montreal and Cambridge (Massachusetts). His PhD work with Ralph Staley at MIT (1981) was on ICR based transition metal ion chemistry. After a postdoc with E. Schumacher and Habilitation in Bern (1987), he became an assistant and then tenured associate professor at Northwestern University in Evanston working on metal clusters and fullerenes. In 1992, he joined U. Karlsruhe-TH (now KIT) as a professor of Physical Chemistry. Since 1998 he holds a joint appointment at the Institute of Nanotechnology.



- (4) In proof-of-principle experiments it has been possible to probe oftentimes quite pronounced conformer/isomer dependencies of physical and chemical properties; such studies are much harder in condensed phase mixtures and additionally complicated by lower interconversion activation barriers;
- (5) Intermediates (and isomers thereof) can be extracted from condensed phase reaction systems (e.g. to study the mechanism of homogeneous catalytic cycles involving the cooperative interaction of two or more TM centers);
- (6) The perturbing environment can be controllably “switched on” by varying the number and orientation of solvent molecules and/or counterions, for example for probing the origins of solvatochromism. In fact many dynamic processes ranging from energy relaxation to chemical reactivity can be probed under conditions ranging from isolated, aggregated to fully solvated – thus also accessing completely new dissipation and reaction channels.

This review focuses on the novel experimental methods enabling such studies by allowing for characterization of isolated molecular ions. Generally, the methods have in common the fragment-free volatilization of typically quite fragile and redox-active molecules by electrospray ionization (ESI) and their characterization by high resolution mass spectrometry. Additionally, the properties of the corresponding ions are characterized by various forms of spectrometry and spectroscopy. The novelty of the approach lies in the hybridization of mass analysis and (oftentimes multi-step) characterization – only one mass-to-charge selected species at a time is probed. Below we discuss how this is done for selected examples and show what the future holds for this general approach – notably isomer specificity.

The review is organized as follows: we begin with a description of ESI-MS as used to generate and characterize the isolated ions of interest and follow this with a section on ion mobility spectrometry (IMS) in particular to probe and select isomer/conformer composition for further study. This also includes a description of the interfacing of IMS with laser spectroscopy. After briefly discussing the use of collision induced dissociation (CID) to quantify – ground state - fragmentation energetics and the application of ion trapping for probes of ion molecule reactions we turn to vibrational spectroscopy. This is carried out in various IR-laser photodissociation and multiple IR photon dissociation approaches – both using one and multicolour schemes including also pump-probe arrangements which allow for the identification and interconversion of isomers. Finally, we turn to electronic spectroscopy both in the frequency and time domain emphasizing the importance of cryogenization and ending with a discussion of the use of X-ray magnetic circular dichroism (XMCD) to probe magnetic coupling in gas-phase oligomeric TM complexes. We finish with some thoughts on future perspectives in this field.

ESI-MS. Mass spectrometry is a well-established analytical method in inorganic and organometallic chemistry. For example electron impact mass spectra of porphyrins and subsequently also transition metal containing metalloporphyrins were re-

ported as long ago as 1965.^[2] However, such studies were limited to sublimable substances. The development of electrospray ionization (ESI) mass spectrometry (MS)^[3] first used mainly for biopolymer analysis, ultimately also led to a significant advance in inorganic mass spectrometry because now fragile, non-sublimable (and often inherently charged) inorganic substances dissolved in polar solvents could also be accessed. Copper phthalocyanine tetrasulfonate, with one transition metal center, was among the first organometallic complexes to be electrosprayed from solution for mass spectrometric analysis in 1989.^[4] This was rapidly followed by ESI-MS of small^[5] (1990)^[6] (1993) and then also larger transition metal cluster complexes (e.g. a 12-atomic ligand stabilized tin cluster^[7] (1994)). In spite of these early pioneering studies, analysis of multi-metal-center inorganic complexes by ESI-MS did not become routine until the early 2000s when chemistry departments started replacing their electron impact- and desorption probe-based mass spectrometers with a new generation of commercial high resolution mass spectrometers equipped with ESI ion sources.^[8] A study of the ligand-stabilized Au₁₈Se₈ cluster system also using ESI-FTMS (Fourier Transform Mass Spectrometry) is a case in point.^[9] These days ESI-MS is commonly used on equal footing with condensed phase analytics towards characterization of novel organometallic syntheses (Figure 1).

The delay in assimilation of ESI-MS by inorganic vs. biochemical mass spectrometry can also be traced back to inherent problems of the ionization method itself. ESI of charged transition metal complexes is often associated with electrochemical redox processes as well as (further) complexation *during the spray process itself*. Such reactions can

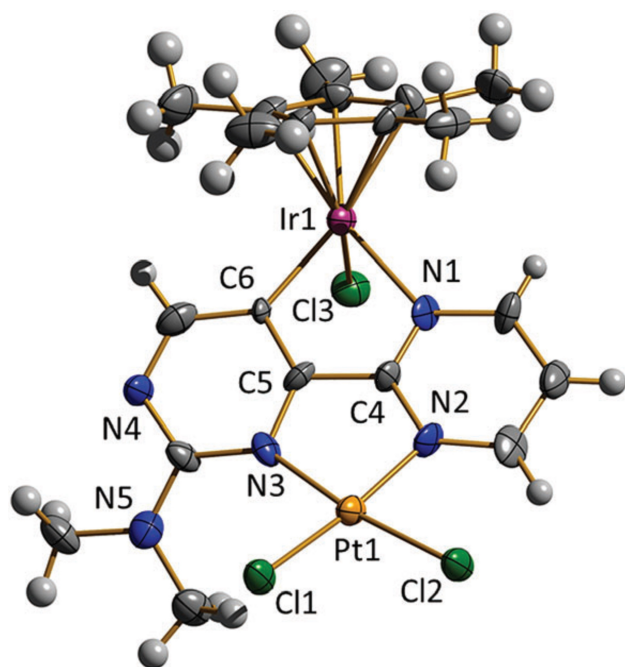


Figure 1. Molecular structure of a neutral Ir^{III}Pt^{II} complex in the solid state. Its bulk phase characterization was augmented and supported by detection of the anionic chloride complex via ESI MS. Reproduced with permission from Ref. [15], Copyright 2021, Wiley-VCH.

dramatically distort mass spectra relative to the abundance distributions of the charged species present in the equilibrium solution. Towards the end of the 2000's it was clearly shown,^[10] that these problems can be reduced by careful control of solution concentrations and by correlating the relative intensities in mass spectra with other solution analysis methods. Then it becomes possible not only to study the kinetics of solution reactions by using ESI-MS to probe reactant and product concentrations^[11] but also to study the *mechanism* by resolving charged intermediates, for example in selected homogeneously catalysed reactions.^[12–16]

ESI-IMS-MS and ESI-MS-IMS-MS: Ion mobility mass spectrometry (IMS-MS) as applied to the structural characterization of molecular ions dates back to the early 1990's.^[17] In its first and conceptually simplest “drift-tube” variant, a DC electric field pulls ions through a collision cell containing an inert collision gas such as helium or nitrogen (at a pressure of a few mbar). The corresponding drift time is measured to yield an ion mobility which is correlated with a specific mass-to-charge (*m/z*) ratio. From this the Mason-Schamp equation can be used to calculate a rotationally averaged experimental collision cross section (^{exp}CCS) for the ion of interest – for comparison with values predicted for various possible structural models (^{theory}CCS).^[18] Ligand-free elemental clusters with completely unknown structures were among the first molecules to which IMS was applied in this way. The corresponding home-built machines combined specialty ion sources (e.g. laser vaporization + supersonic expansion) with custom helium filled drift-tube setups. Because of the innate polydispersity of the species generated in the gas-phase cluster sources, early machines were of the MS-IMS-MS type, i.e. the cluster ion of interest was mass-selected prior to the mobility measurement and the absence of fragmentation was then checked for in a further mass measurement subsequent to drift tube passage.

The first ESI-MS-IMS-MS setup was implemented in 1995.^[19] Apart from the ESI ion source, it made use of essentially the same apparatus configuration as developed earlier for cluster studies. ESI-MS-IMS-MS was initially used to document and study the often multiple coexisting conformations of isolated biopolymer ions in gas-phase. Driven by applications in mass spectrometry-based protein and DNA sequencing, the method was then applied towards exploring how the isomeric structures of a range of different biopolymers depended on excess charge. At the time, fragile transition metal cluster complexes were just beginning to be accessed for analytical ESI-MS (see previous section). It took more than five more years before the first ESI-MS-IMS-MS studies of ligand stabilized multicenter transition metal cluster complexes appeared. As an example, Weis et al.^[20] reported in 2002 ion mobility measurements of the Au₁₈Se₈ cluster mentioned above (including fragments thereof).

Since the mid 2000's the field of ESI-(MS)-IMS-MS has exploded due both to the development of improved IMS methods and *in particular due to the commercialization of the corresponding IMS-MS technologies*.^[21] Arguably, this started with the introduction of the Waters Synapt G2 instrument (based on travelling wave ion mobility mass spectrometry (TWIMS)) (2006). There followed the Agilent IM-Q-TOF setup (Drift tube ion

mobility) (2014) and then the Bruker TIMS-TOFMS apparatus (trapped ion mobility) (2016).^[21] The recently introduced Waters Cyclis-IMS (2019) instrument has continued the series of new commercial platforms with further increased mobility resolution.^[22] Nowadays ion mobility resolutions near 200 (CCS/ Δ CCS) can be routinely achieved using several different commercial platforms operating with nitrogen collision gas. Systems with even higher mobility resolutions of ca. 10^3 are presently under development.

The present generation of high resolution ESI-(MS)-IMS-MS machines also achieves absolute CCS accuracies, i.e. reproducibility in CCS values, of significantly better than 0.5%. This is made possible not only by mechanically robust construction but also by taking into account systematic error sources such as fluctuations in drift gas temperature or pressure by calibrating measured ion mobilities against molecular standards (e.g. Agilent "Tunemix").

The increasingly higher levels of accuracy and resolution in CCS determinations by IMS allows improved differentiation of the shapes of large organometallic ions in isolation – for example to resolve, multiple (non-interconverting) conformers or isomers (Figure 2). Deeper structural insight involves translating the corresponding experimental ^{exp}CCS values into molecular geometries by fitting them to values predicted for plausible structural models, ^{theor}CCS. The presently highest level of such CCS modelling involves coupling DFT calculations with trajectory calculations (as for example implemented in the IMoS program^[23]) to describe scattering of collision gas molecules/atoms with the ions in question. Work is ongoing to further improve several aspects of this process: (i) DFT trial geometries are typically based on starting coordinates derived from condensed phase structures (e.g., from X-ray crystallography). These must be optimized to approximate the true gas-phase geometries free of matrix effects. Often, particularly for large systems, this requires inclusion of dispersion interactions which in quantum chemistry packages have so far been parameterized

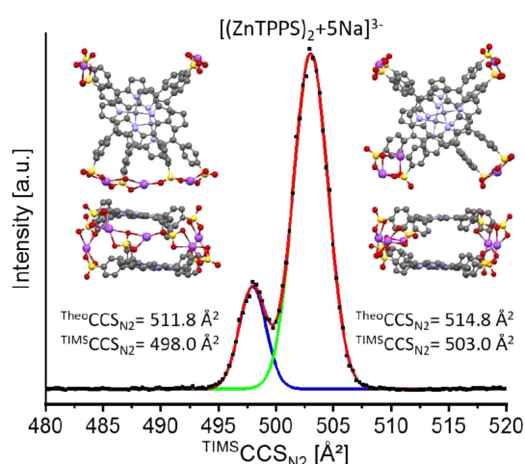


Figure 2. High resolution ion mobility measurement (TIMS) resolving two different counterion adducts of cofacial tetraphenylsulfonato zinc porphyrin dimers (shown respectively in both front and side views (unpublished, E. Schneider and M. M. Kappes)).

only using condensed phase structural data - thus leading to overcompensation effects; (ii) trajectory-method calculations make use of two-body collision gas...ion interaction potentials which typically comprise sums of element-specific van der Waals-, charge induced dipole- and ion quadrupole- interaction terms. For many elements, in particular transition metals and lanthanides, the corresponding van der Waals parameters have yet to be determined/optimized. Similarly, charge partitioning among the atoms of specific DFT output structures optionally makes use of several different possible procedures. These remain unvalidated for IMS applications, i.e. it is not clear which to choose to best model the real charge distributions. (iii) Finally, the experiment probes a thermalized ensemble whereas DFT calculations are vibrationless. Ultimately, integrated numerical approaches including MD treatments are required to better take temperature into account – but such efforts are generally still in their infancy.

Consequently, even if the correct isolated ion structure has been found by DFT, agreement between the CCS simulation thereof based on trajectory calculations and the experimental CCS can vary significantly from system to system depending on the structural rigidity of the molecular ions in question, their overall shape (compact \leftrightarrow open), bonding properties, charge localization and size. For example, deviations between timS-TOFMS experiment and best fitting CCS simulations of organometallic complexes so far studied in 3MET have ranged from below 1% to greater than 10%. Nevertheless, as the "training set" of rigid organometallic molecules with well-known gas-phase structures increases, we expect that the magnitude of such ^{exp}CCS \leftrightarrow ^{theor}CCS discrepancies can be reduced, for example, by optimizing interaction potentials for trajectory-method calculations and/or by using machine learning approaches.

Presently therefore, the power of high resolution ESI-(MS)-IMS-MS lies not so much in the "inverse determination" of the exact gas-phase molecular ion structures, instead it is more useful for distinguishing (and separating) the different isomeric shapes present after electrospraying.^[24] In this context it is important to realize, that the barriers to conformer interconversion are typically much larger in gas-phase than in solution. Thus ESI-IMS can potentially serve to "freeze out" parts of the conformer space which would otherwise be too rapidly sampled by solvated molecules in room temperature solutions. Along the same lines, structurally distinct adducts of counterions (e.g. Na⁺) with a molecular ion (Mⁿ⁻) having multiple localized charges – $[M(Na)_{n-m}]^{m-}$ may be distinguishable by IMS-MS. Thus, their relative intensities and CCS values can be used for topological analyses of the "labelled" molecular ions. Also, specific counterion adduct "isomers" can be selected by ESI-IMS for further study, for example for probing the influence of (static) electric fields on optical properties.

(ESI-)IMS and tandem IMS-IMS methods are increasingly also being used to probe isomer interconversion (rates) – so far primarily of biopolymer ions, for example^[25] Most of the corresponding experiments have been performed using ion mobility cells held at or near room temperature – although in several cases temperature variable drift tube setups have also

been constructed, for example T-dependence of isomer inter-conversion rates is also relevant for spectroscopy of isomers separated by room temperature IMS and then trapped and cooled to cryogenic temperatures (as described below).^[26,27]

Interfacing ESI-(MS)-IMS-MS with laser spectroscopy: Mass- and mobility-resolved laser spectroscopy of molecular ions, i.e. “hybrid” MS in serial spatial/temporal combination with IMS and laser spectroscopy, was first demonstrated in 2002.^[28] This study reported isomer-specific photoelectron spectra of small carbon cluster anions generated by a pulsed arc discharge source (PACIS). It used helium drift tube ion mobility to separate the chain from ring carbon cluster anion forms (which are formed simultaneously) followed by mass selection and photoelectron spectroscopy, PACIS-IMS-MS-PES. Analogously isomer-resolved electronic photodissociation spectra of carbon cluster cations (in this case generated by laser vaporization (LV)), were reported in 2009, LV-IMS-PD-MS.^[29] The custom setups used for these two pioneering studies consisted of short IM drift tubes combined with comparatively low collision gas pressures to maximize ion transmission (>0.1%) and thus maximize signal levels for the corresponding spectroscopic measurements. As ion mobility resolution scales with drift tube length this was necessarily associated with low mobility resolutions – still sufficient however to distinguish the unusually dramatic CCS difference between carbon rings and chains.

A solution to the dilemma of decreasing signal intensity versus increasing mobility resolution by collisions with a drift gas was provided in 2005 by the implementation of hydrodynamic ion funnel interfaces for ESI-IMS-MS – both at the inlet and outlet of the IMS drift tube. Ion funnels are optimized for operation at the mbar pressures typically used in drift tube IMS and enhance transmission of ions tremendously – such that much longer drift tubes and correspondingly higher resolution separations became possible prior to spectroscopy.^[31] Consequently in 2011 (coinciding with the beginning of 3MET funding) the first ESI-IMS based machine to be built for isomer-resolved spectroscopy also incorporated two such ion funnels. This apparatus was initially configured for photoelectron spectroscopy, ESI-IMS-MS-PES, and first applied to isomers of DNA oligonucleotide multianions.^[32] It provides for a mobility resolving power (in helium) of ca. 45–50. Since then the machine has also been applied to study several different 3MET systems, including PES of coplanar vs. cofacial, non-covalently linked metalloporphyrin dimers.^[33] More recently the apparatus was extended to also allow for isomer resolved electronic photodissociation (PD) spectroscopy of near room temperature ions (with mass-specific detection of fragments), ESI-IMS-MS-PD-MS^[30] – Figure 3.

Since the first demonstration of ESI-IMS-MS-PES in 2011, the field of ion spectroscopy of ESI-IMS preselected isomers/conformers has developed rapidly to include several new or significantly improved apparatus variants, for example: (i) electronic photodissociation spectroscopy of preselected ions stored (and thermalized) in a cryo-cooled ion trap, ESI-IMS-MS-cryoPD-MS,^[34] (ii) infrared multiple photon photodissociation spectroscopy (IR-MPD) of mobility selected ions using a high

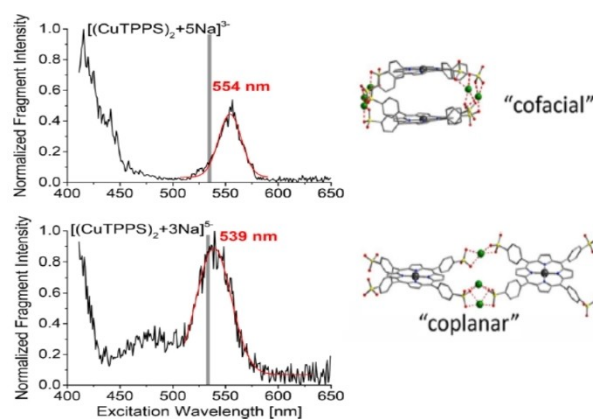


Figure 3. ESI-IMS-PD-MS measurements of the Q-band electronic absorption regions of selected copper porphyrin dimer multianion topographies: cofacial versus coplanar. Gray vertical lines: TD-DFT predictions. Reproduced with permission from Ref. [30], Copyright 2021, Wiley-VCH.

intensity free-electron laser, ESI-IMS-MS-IRMPD-MS,^[35] (iii) ESI-tandem IMS-IMS coupled to laser excitation for photodissociation or photoisomerization studies requiring structure separation/analysis both before and after the photoexcitation stage^[36] and,^[37] ESI-IMS-PD-IMS-MS. Most recently, (iv), the new ultrahigh mobility resolution technique “structures for lossless ion manipulation (SLIM)” has also been implemented for tandem IMS in combination with cryo photodissociation spectroscopy, ESI-IMS-CID-IMS-MS-cryoPD-MS.^[38]

Now that both long term ion trapping and ion mobility separation have become essentially lossless, it is clear that the future will hold many interesting further possibilities for hybrid ESI-IMS-MS methods and their chemical applications. Here in particular photonic interactions provide promising options for further elucidation.

Collision Induced Dissociation (CID): Perhaps a little more “old-fashioned” than the novel IMS-based techniques described above, Collision Induced Dissociation (CID) has been a workhorse of gas phase ion chemistry for many decades. In CID, statistical analysis of the fragmentation dynamics enables quantification of binding energies in a well-established way.^[39] However, this type of approach can run into problems for cases where reliable quantum state counting becomes questionable as for example for larger complexes of multiple TM centers. Then, it may no longer be feasible to extract quantitative bond dissociation energies from an analysis of CID thresholds. This can become even more of a problem when the strict requirement of CID measurements, i.e. single collision conditions at well-defined collision energies is no longer fulfilled, for example when conducting measurements within RF ion traps. In such cases it is nevertheless gratifying to realize, that *relative* values of recorded fragmentation thresholds can still be useful for the interpretation of relative stabilities, for example of Au–Zn–Alkali Complexes,^[40] or in magnetostructural correlations within Fe₃O-(ac)₆⁺ and its complexes with n-heterocycles.^[41] Likewise, the elucidation of roll-over cyclometallation within Ru^{II}

complexes,^[42] and further related studies have benefitted from such CID studies and their corresponding interpretation.^[43]

Despite being able to routinely determine relative CID thresholds under such conditions it remains beneficial to search for calibration methods to transform these to absolute bond dissociation energies. In this regard it has proven helpful to rely on so called “thermometer ions”, for example benzylpyridinium substituted porphyrins.^[44] The breakdown curves of these ions show a linear correlation between experimental fragmentation thresholds (in instrumental units of “normalized collision energy”) and theoretical dissociation energies, confirming that these species can be used as calibrants to gauge the fragmentation energetics of closely related systems. However, thermometer ions need to be taken with a grain of salt when interpolating among systems of vastly different densities of states.

From Chemistry in Ion Traps to Spectroscopy of Educts, Products and Intermediates: The advent of TM ion chemistry studies in room temperature Ion Cyclotron Resonance (ICR) ion traps dates back more than 40 years.^[45,46] Coupling of ion chemistry probes with synchrotron and laser spectroscopy within such ICR ion traps and at cryo temperatures is more recent.^[47–49]

In the meantime, ICR studies have also been complemented by ion beam probes in conjunction with RF ion guides.^[50–52] Such technology enables meticulous studies of activated processes at TM clusters, and allows to extract archival values of many thermodynamic properties such as binding enthalpies, and to apply thermodynamic cycles to transfer this knowledge to the determination of further energetic quantities in a consistent way.^[39,53–57]

A large part of these and numerous other reactivity studies of TM clusters were reviewed before, with an emphasis on additivity, cooperativity, many body effects, synergism and cluster size scaling laws.^[58] For example, it became possible to conduct TM gas phase ion reactivity studies with binary gas mixtures, and to fingerprint catalytic cycles as mediated by small clusters of Gold, Silver and Platinum.^[59–64]

The reactivity of ESI isolated TM complexes has also been characterized in RF or ICR ion traps in conjunction with some spectroscopic elucidation and partly under cryogenic conditions.^[65–72] A high temperature linear ion trap reactor design^[73] proved useful for characterizing the reactivity and catalytic activity of oligomeric TM compounds,^[74,75] and it helped to survey Rhodium cluster chemistry^[76] and N₂ activation by some of these oligomeric TM compounds.^[77–80] Independently, the room temperature size-dependence of the reactivity of tantalum cluster cations with small alcohols has received some attention.^[81]

All of these reactivity studies – valuable and insightful in their own right – made obvious the pressing need for further spectroscopic characterization, and in some cases have begun to address it. The route towards isomer selective spectroscopy of reaction intermediates and products shall be described in the next section.

One and two colour IR and tagging techniques: Infrared spectroscopy is in itself a well-established and eminently useful

tool for the elucidation of molecular structures. Yet, it often suffers from limitations and interferences which stem from the molecular environment. Isolation helps and therefore the capability of conducting IR spectroscopy on well-defined molecular ions in isolation was a long hoped for advance. Such vibrational spectroscopy of isolated molecular ions was made possible through the combination of tunable InfraRed-Multiple-Photon-Dissociation (IR-MPD) with dedicated tandem mass spectrometry and RF ion trapping.^[82,83] This started an evolution of this new field towards a wide range of topics as reviewed before.^[84–88] This development has benefitted extremely from the advent of what are arguably the two most innovative types of IR laser instrumentation: OPO/OPA lasers as marketed by LaserVision^[89] made the “stretching frequency” range (2200–4000 cm⁻¹) accessible at high spectral resolution (2 cm⁻¹ and better); additionally the “fingerprint” spectral range (660–2000 cm⁻¹) became available by subsequent difference frequency mixing (DFM). In parallel, the large-scale instrumentation platform of Free Electron Lasers (FEL) was adapted to allow for high flux and tunable IR photon generation over even wider spectral ranges, and in particular down to 200 cm⁻¹ and below. There are presently three IR-FEL sites, all in Europe: CLIO near Paris,^[90] FELIX now at Nijmegen^[91] and the FHI-FEL in Berlin.^[92] Two of them (CLIO and FELIX) operate as user facilities. In particular in the spectral ranges which are also accessible to table-top OPO/OPA systems, the applicability of IR-FELs to the study of oligonuclear transition metal compounds suffers somewhat from their significantly larger laser bandwidths of typically 1% of the photon energy.

IR-MPD is a type of action (or depletion) spectroscopy. Thus, predicting and understanding the relation of recorded band intensities to the intrinsic IR absorption strengths is non-trivial and remains an ongoing research issue. Often, the correspondence is close, sometimes the relation is nonlinear, and in some other “worst” cases, bands predicted in quantum chemical calculations are totally missing in the corresponding IR-MPD spectra. At this writing, there is a general but still mainly qualitative understanding of this phenomenon in terms of sparse density of states and the mode specific magnitudes of anharmonic couplings.^[93,94]

It became clear soon after introduction of the IR-MPD method, that action spectroscopy does not suffer from such problems in cases for which the photon energy and dissociation threshold compare favourably (i.e. when the former is significantly greater than the latter). This favourable situation was initially recognized for charged hydrogen clusters.^[95,96] and led to the development of various types of IR-PD tagging spectroscopies, invoking weakly bound messengers such as H₂, Ar, Ne, He, or N₂. Thus, it became possible to conduct Infra Red Photon Dissociation (IR-PD) spectroscopy with *single* photons, but at the dual expense of necessary cryo conditions and of attached weakly perturbing messengers.^[97,98] In parallel, the increasing availability of FEL beamtime enabled numerous IR-MPD studies of TM compounds largely devoid of “dark band” deficiencies.^[99] The value of tunable IR-MPD was also realized by the MS bioanalytics community, for example by conducting IR-MPD

spectroscopy of electrosprayed ions when trapped in a Fourier transform mass spectrometer.^[100]

IR-PD and IR-MPD studies of specific TM compounds have greatly aided understanding of their bonding properties (Figure 4) but the overall impact of these methods on the field of coordination chemistry has been hampered by the fact that none of these techniques have yet become routine (in the sense that they rely on custom rather than commercialized instrumentation). Nevertheless, a more recent achievement has opened new perspectives for more widespread investigations. Specifically, the combination of two colours of IR photons gives rise to novel opportunities in action spectroscopy, for example to selectively probe coexisting isomers and conformers. The technique of two-colour IR-MPD has been applied to TM compounds from its very beginnings.

Inevitably, the one colour IR-PD and IR-MPD efficiencies of untagged complexes decline exponentially towards low photon

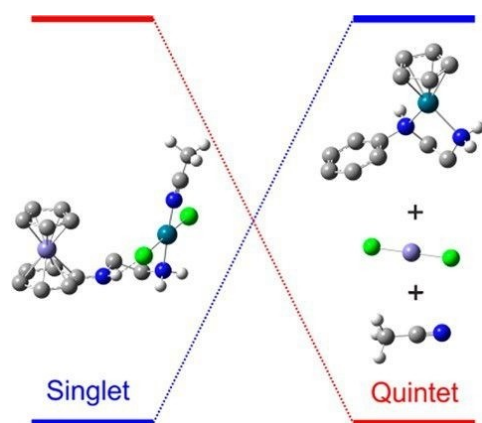


Figure 4. A combination of ESI-MS with IR action spectroscopy and DFT modelling was used to probe direct singlet – quintet state coupling in the course of a chlorido and Cp ligand exchange among the Fe and Pd metallic centers. The method combination answered the question of how this occurs: in a concerted, ballet-like manner, transforming a coordinated PdCl_2 motif into a FeCl_2 leaving group. Reproduced with permission from Ref. [13], Copyright 2021, Wiley-VCH.

energies. Whereas in early work the onset of significant non-linear damping of IR-MPD yield versus expected (and sometimes computed) IR activities was found to set in at about 3000 cm^{-1} ,^[101] improved table top laser instrumentation shifted this operational limit to below 1200 cm^{-1} ^[102–103] and in the most favourable cases as low as 660 cm^{-1} .^[104] Nevertheless, the required balance between weakest bond energy, oscillator strength and necessary photon flux (total energy per few nanosec laser pulse) oftentimes remains unpredictable and often causes weak IR bands to disappear in IR-MPD spectra.

Recently a sequence of two IR pulses at different frequencies has been applied to trapped ion packages: the first pulse serves to scan the fingerprint region, whereas the subsequent second pulse is tuned to a strong stretching mode resonance so as to enhance the IR-PD yield. It proved imperative to attenuate the photon flux of the enhancing second pulse so as to induce essentially no fragmentation of its own. Thus, the prior frequency-tuned pulse makes up for the otherwise missing amount of excitation and gives rise to a spectral fingerprint – the IR adsorption profile – which is related close to linearly with the recorded fragmentation yield. Early application examples of this two-colour infrared photo dissociation (2cIR-PD) method were the characterization of a dimeric silver complex uncovering a Hoogsteen-type, nucleobase-mimic coordination motif (Figure 5)^[105] as well as a study of dimeric silver complexes of 1-methylthymine.^[102] Also, a multi method characterization of a Ruthenium transfer hydrogenation catalyst of the type $[(\eta^6\text{-cym})\text{RuX}(\text{pympyr})]^+$, benefitted from 2cIR-PD spectra of precursors (before HCl loss) and of activated complexes (after HCl loss), and it eventually become possible to elucidate C–H activation as the key step in the activation mechanism.^[106] Likewise, the structural characterization of Thymine-Uracil-Tetracyano- Pt^{II} -Aggregates benefitted strongly from 2cIR-PD spectra together with DFT modelling that revealed decisive bands below 1500 cm^{-1} , as opposed to previous 1cIR-PD attempts.^[107]

While these applications of the 2cIR-PD scheme aimed at mere signal enhancement, it proved possible to extract further information from such experiments by varying pulse sequence

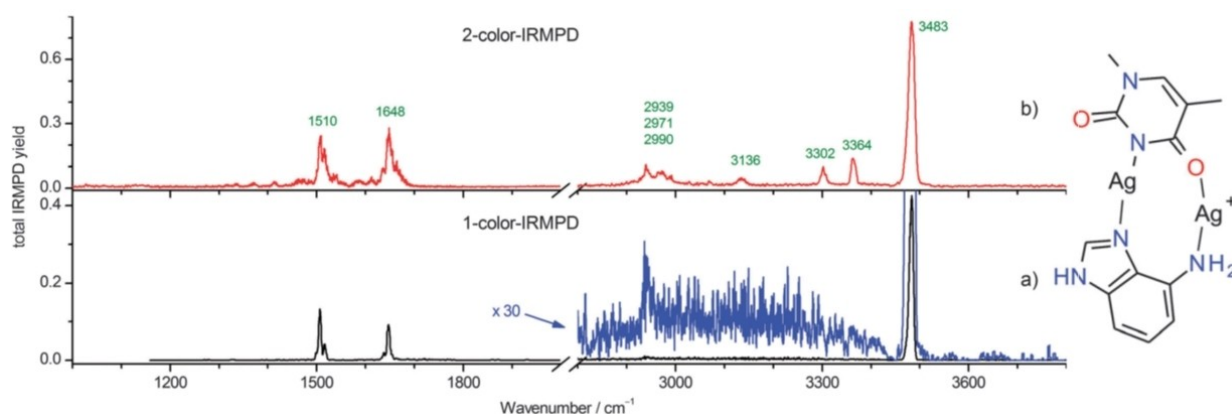


Figure 5. The two colour enhanced 2cIR-PD spectrum of a $[(\text{Ag})_2(1\text{MT-H})(\text{DDA})]^+$ complex (a) allowed for the identification of a Hoogsteen type binding motif (inset), while the conventional one colour IRMPD spectrum (b) failed to elucidate several IR active bands. Modified with permission from Ref. [105], Copyright 2021, Wiley-VCH.

and interpulse delay. Of course, 2cIR-PD with nanosec pulsed laser sources cannot be used to study ultrafast dynamics. However, reversal of pump and probe pulse sequence provides additional insight by allowing a comparison between the pristine complex and the same complex activated by a pump pulse. This was shown in a study of a mononuclear Ag(I) complex with two coordinating ligands: *o*-cyano-4-hydroxycinnamic acid ($\text{HCCA}=\text{L}_1$, monodentate ligand) and 2-(5-methyl-1H-pyrazol-3-yl)pyridine-16 ($\text{MPP}=\text{L}_2$, bidentate chelate).^[108] The resulting $[\text{AgL}_1\text{L}_2]^+$ complex serves as a model for ligand-to-chelate hydrogen bonding within a “ligand-metal-chelate” complex and for a possible torsional isomerization, in which isomer A (Figure 6) stabilizes through a NH–O hydrogen bond and isomer B through a CH–O hydrogen bond leaving the NH chromophore dangling. Probing the phenolic OH with a pulse 200 ns after the scanning pump pulse reveals significant population of the more stable isomer A (–8 kJ/mol with respect to B) through the fingerprint of the H-bound NH oscillator around 3400 cm^{-1} (cf. red trace in Figure 6). This feature is absent when sending in the probing pulse first at –100 ns and subsequently irradiating with the scanning pump pulse (blue trace). In line with valuable insights from DFT modelling these 2cIR-PD results proved the concept of isomer probing, which was subsequently widely applied, examples of which will be discussed in the following.

Most recently, N_2 -tagging cryogenic infrared photon dissociation (IR-PD) experiments at 40 K have been used to investigate dinuclear coinage metal phosphine complexes with attached hydrogen oxalate ($(\text{CO}_2)_2\text{H}=\text{HOx}$), of the form $\text{M}_1\text{M}_2\text{dcpm}_2(\text{HOx})$ with $\text{M}=\text{Cu}, \text{Ag}$ and $\text{dcpm}=\text{bis}(\text{dicyclohexyl-phosphino})\text{methane}$, abbreviated $[\text{MM}]^+$.^[109] These studies revealed spectral patterns of the structural motifs at play in HOx isomers that differ according to the binding motifs to the bimetallic center, assigning three isomers of $[\text{CuCu}]^+$ and four isomers of $[\text{AgAg}]^+$. Isomer-specific 2c IR-PD hole burning experiments

showed that the recorded attenuations of vibrational band patterns are indeed isomer specific and allow to estimate the magnitude of isomerization qualitatively (Figure 7). The isomeric interconversion proved considerable in cryogenized $[\text{AgAg}]^+$ upon IR activation, and it seems largely absent in the corresponding $[\text{CuCu}]^+$ complexes. These findings indicate that HOx undergoes stiff coordination in $[\text{CuCu}]^+$ but more flexible coordination in $[\text{AgAg}]^+$.

While cryo tagging spectroscopy can presently achieve high sensitivity in such frequency ranges as well, the experimental effort involved with cryo trapping and messenger tagging remains significant. In contrast, the 2cIR-PD technique is perhaps more readily applicable: it involves standardized MS equipment in combination with nowadays standardized table top laser equipment without further instrumental modifications.

Most noteworthy in this context are also applications of isomer-specific 2cIR-IR Double Resonance Spectroscopy beyond TM complexes, such as for example of D_2 -tagged protonated dipeptides as prepared in a cryogenic ion trap,^[111] of coexisting Eigen and Zundel cations in the case of protonated water clusters^[110] (Figure 8) or the systematic investigation of spectral diffusion in hydrogen bonded networks.^[112] A full coverage would be beyond the scope of the current review. Also a large fraction of such work has been covered by two recent reviews.^[99,113]

There are cases where neither isomeric mixtures nor IR induced isomerization dynamics are of importance. Instead it is of interest to identify some prevailing conformation(s) along an assumed or suggested reaction path. Most recently, the activation of N_2 by small clusters of tantalum and vanadium has come into the focus of multiple studies.^[114–116] Obviously, it takes more than a single metal center to activate N_2 . In which way this might take place has been subject of debate and any insight in this regard is most welcome. Neither the currently possible types of experimental investigations nor quantum

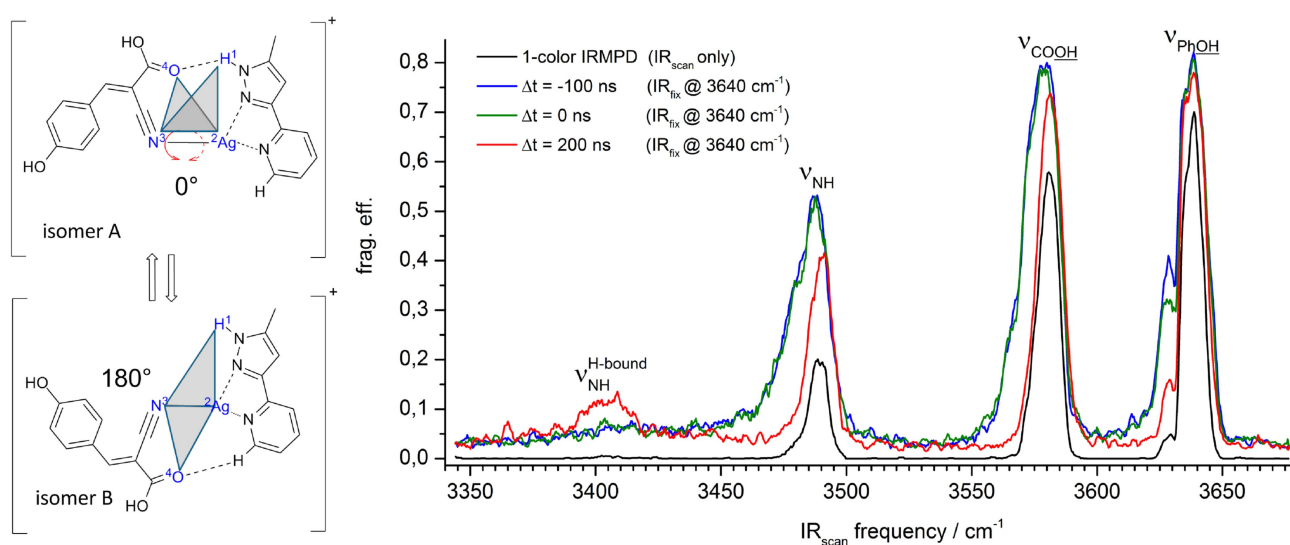


Figure 6. Torsional isomerization within a $[\text{AgL}_1\text{L}_2]^+$ type complex (left) may signify through the H binding induced shift of an otherwise free NH oscillator. 2cIR-PD measurements verified this idea by reversal of the sequence of pulses (right). Modified with permission from Ref. [108], Copyright 2021, Wiley-VCH.

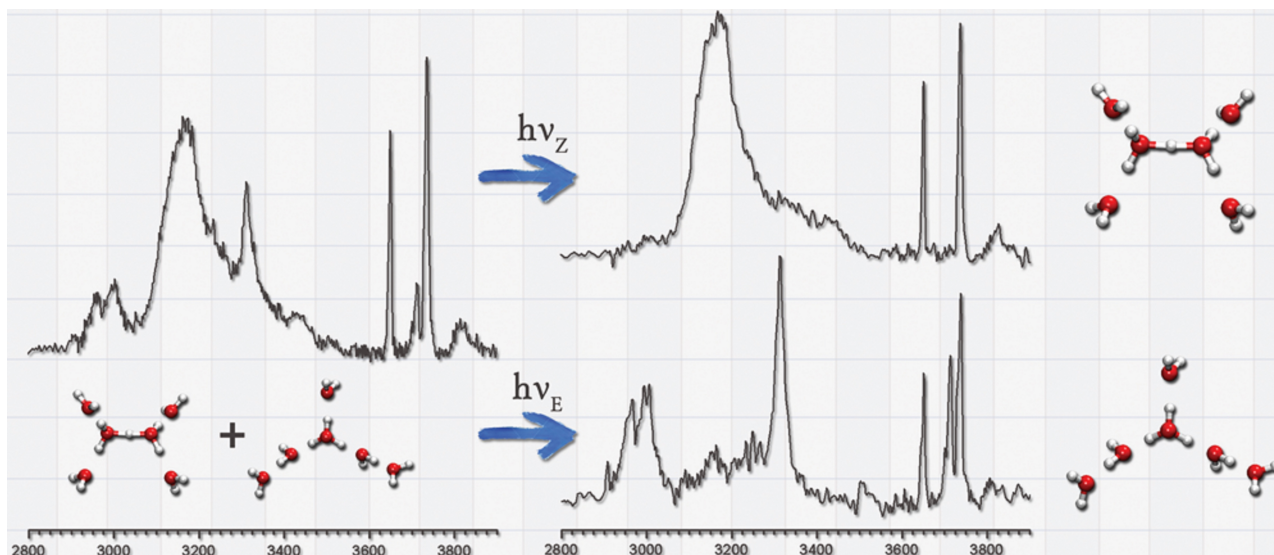


Figure 8. The IR depletion spectrum of mass-selected $\text{H}^+(\text{H}_2\text{O})_5\text{H}_2$ complexes (left) is unravelled into its two contributions by 2cIRPD probing at 3167 cm^{-1} (right, top) which is characteristic of H_5O_2^+ Zundel cation moieties, and at 3714 cm^{-1} (right, bottom) which is characteristic of H_3O^+ Eigen cation moieties. Reproduced with permission from Ref. [110], Copyright 2021, Wiley-VCH.

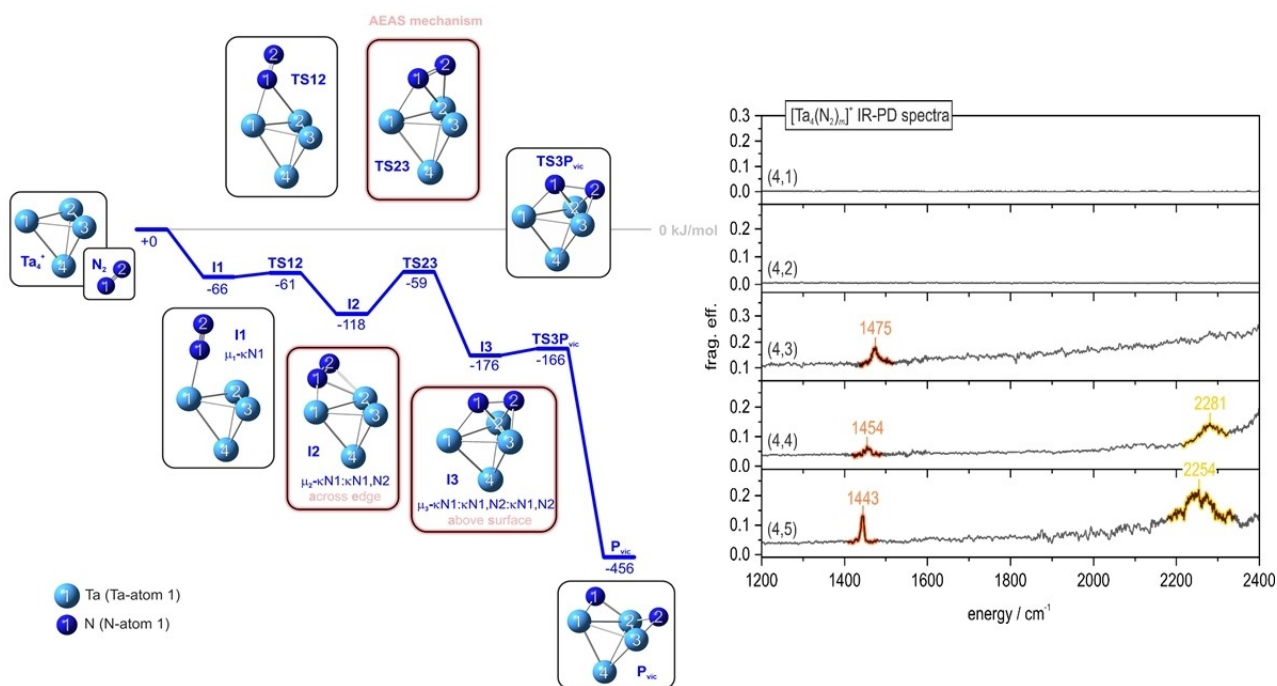


Figure 9. The activation of a first N_2 by Ta_4^+ proceeds in a multi-step “across edge above surface” (AEAS) process across submerged barriers (left), likewise for a second N_2 . A third N_2 activation gets stuck at the “across edge” I2 intermediate, which is signified by its characteristic IR-PD N_2 stretching band around 1475 cm^{-1} (right). Reproduced with permission from Ref. [117], Copyright 2021, Wiley-VCH.

ultraviolet detection, at that time termed resonant two photon ionisation (R2PI).^[120] Much has been done with these methods to study organic and biochemical compounds, for example peptides and biomimetics and as reviewed recently.^[121] Few TM complexes have been investigated with such schemes. The R2PI method in itself has of course been systematically and extensively applied for the determination of bond dissociation

energies of various heterogeneous TM dimers and related compounds in isolation.^[122]

Electronic excitations: statics and dynamics: While the photophysics of oligonuclear TM compounds has been extensively characterized in condensed phase, corresponding electronic spectroscopy studies of isolated gas phase species are rarer (see also IMS section above) particularly as related to time-

resolved measurements. A noteworthy example elucidated the dynamics of a silver dimer chloride scaffold which was stabilized by two bidentate phosphino methane ligands, $[\text{Ag}_2(\text{Cl})(\text{dcpm})_2]^+$ ($\text{dcpm} = \text{bis}(\text{-dicyclohexylphosphino})\text{methane}$).^[123] Photoexcitation by an ultraviolet pulse induces a coherent vibrational wave packet motion in the excited state that was probed by a subsequent second pulse through ionization. It was found that the recorded intensities of competing fragmentation channels bear fingerprints of that vibrational motion, cf. Figure 10: In conjunction with quantum chemical modelling the Ag–Ag stretching motion was identified as the origin of the observed 75 cm^{-1} coherence. Moreover, it showed, that the squeezing of the Ag–Ag bond distance towards the inner turning point seems to favour the expulsion of the bridging chloride ligand while the stretching motion towards the outer turning point favours fragmentation by loss of a dcpm ligand. Such fragmentation control by coherent wave packet motion is a rare observation in continuation of early work on the ligand-free sodium dimer,^[124] and provides insights towards new routes of photocatalysis. Along the same lines: analogous investigations of isolated oligonuclear TM complexes often yield surprising results, such as for example the quenching of well characterized and understood lanthanide luminescence upon embedding into a larger scaffold together with Mn^{II} cations.^[125]

Gaseous ion PD spectroscopy, often in combination with messenger tagging, has also been used extensively to study the electronic spectroscopy of various coinage metal cluster systems. An intriguing recent example of PD spectroscopy in

the UV-vis spectral range was obtained for the isolated Au_2^+ cation.^[126] This study at unusually high spectral resolution revealed two vibrationally resolved band systems at 440 and 325 nm with irregular structure. The presumed spin-orbit coupling was confirmed by high-level quantum chemical multi-reference calculations that identified contributions from multiple electronic states. In contrast, simplified modelling with for example widespread DFT methods would have failed. Most recently this type of study has been extended further by recording NIR spectra of argon tagged complexes, Au_2Ar^+ , which revealed long and resolved progressions of Au–Au and Au–Ar stretching modes.^[127]

Light absorption by isolated, metal containing ions can also be accompanied by photoluminescence. If competing dissipative processes such as PD can be made slow enough, for example by collisional cooling, it becomes possible to measure PL emission spectra for selected excitation wavelengths by accumulating signal over multiple absorption/photoluminescence cycles of the same (unfragmented) ion ensemble. Examples include luminescence spectra recorded for mass selected and isolated nonanuclear Lanthanide complexes $[\text{Ln}_9(\text{PLN})_{16}(\text{OH})_{10}]^+$, $\text{Ln} = \text{Eu}^{\text{III}}, \text{Gd}^{\text{III}}$; PLN = deprotonated 9-oxophenalen-1-one, after UV excitation. Whereas the europium complex reveals Eu^{III} -centered emission (Figure 11) sensitized via PLN-based triplet states, the Gd^{III} compound cannot undergo the corresponding ligand to metal energy transfer and just shows a broad ligand-based triplet emission. Both complexes

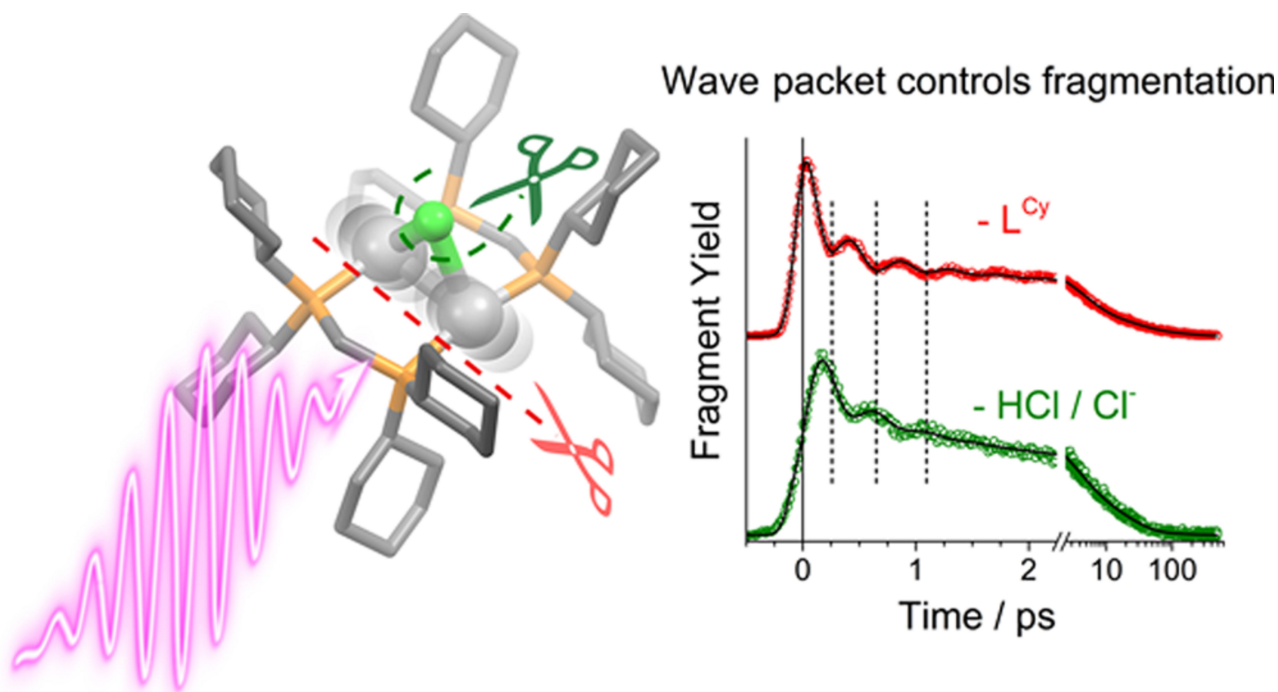


Figure 10. Pump-probe fragmentation action spectroscopy of isolated $[\text{Ag}_2(\text{Cl})(\text{dcpm})_2]^+$ ($\text{dcpm} = \text{bis}(\text{-dicyclohexylphosphino})\text{methane}$) (left) and the observed excited state vibrational coherence of competing fragmentation channels (right). After photoexcitation by an 1XMCT transition (260 nm) in an ion trap, there is an unexpected correlation of specific fragment ions, loss of HCl vs. loss of $\text{dcpm} = \text{L}^{\text{cy}}$. The observed coherences of about 75 cm^{-1} relate to Ag–Ag stretching such that the fragmentation pathways switch at the classical turning points. Reproduced with permission from Ref. [123], Copyright 2021, Wiley-VCH.

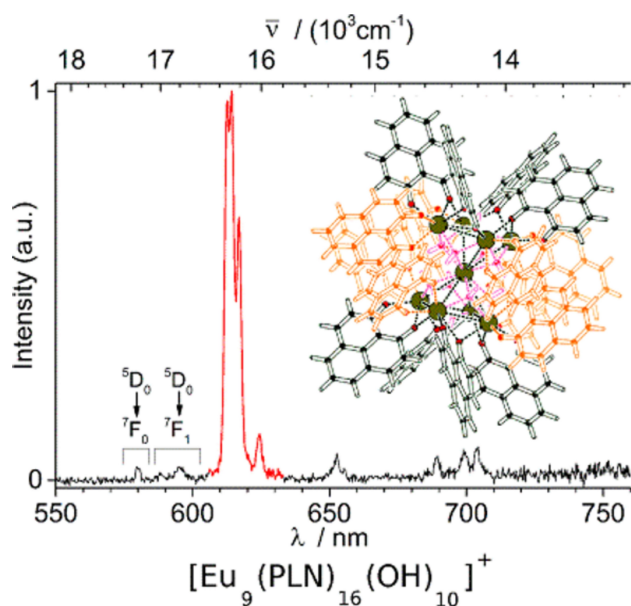


Figure 11. Luminescence spectrum and structure of a nonanuclear europium complex $[\text{Eu}_9(\text{PLN})_{16}(\text{OH})_{10}]^+$. The europium-centered emission after UV excitation results from coupling (and energy transfer) between PLN and Eu^{III} , for details see text. Reproduced with permission from Ref. [128], Copyright 2021, Wiley-VCH.

assume the same square antiprismatic lanthanide core structure.^[128]

Static photoelectron spectroscopy (PES) as well as femtosecond time-resolved pump-probe photoelectron spectroscopy (tr-PES) of individual complexes and clusters necessarily takes place in gas phase only. tr-PES has been mainly applied to neutral and singly negatively charged ions. It is an interesting idea to extend the scheme to di- and multi-anionic species because the associated repulsive Coulomb barriers allow for novel excited state dynamics in some senses complementary to photoluminescence.^[129,130] This was recently done, for example for several dimeric TM compounds, notably gaseous $[\text{Pt}_2(\mu\text{-P}_2\text{O}_5\text{H}_2)_4 + 2\text{H}]^{2-}$, also known as $\text{Pt}_2\text{POP}_4^{2-}$.^[131] In gas phase a significant fraction of the isolated dianions transferred into their first excited singlet state by light absorption decays biexponentially by fast electron tunnelling through a repulsive Coulomb and much more slowly by detachment from a triplet after intersystem crossing. By contrast the same system shows photoluminescence in condensed phase. (Figure 12)

Gas phase XMCD: The elucidation of magnetic couplings amongst unpaired spins at adjacent open d shell metal centers within oligonuclear TM coordination compounds is presently an active research area. Interestingly, while these couplings are weak as compared to covalent or even van der Waals interactions, one of the most appropriate means for their spectroscopic characterization involves high photon energies in the X-ray range. This is only a seeming contradiction. In fact, inner shell excitations can be used for valence shell characterization: the inner shell *p* orbitals are well defined, localized and atomic like with little or no overlap to neighbouring atoms. In contrast, occupied valence shell orbitals – let us say occupied *d*

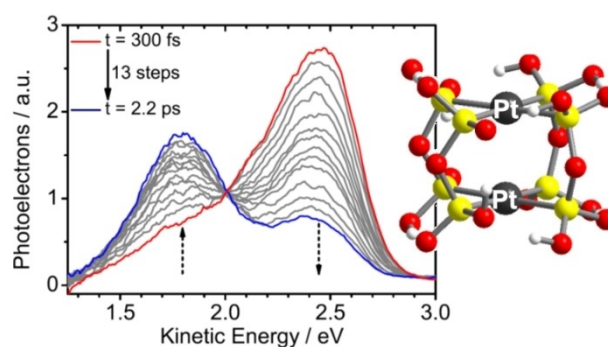


Figure 12. Transient photoelectron spectra and structure of $[\text{Pt}_2(\mu\text{-P}_2\text{O}_5\text{H}_2)_4 + 2\text{H}]^{2-}$. The isosbestic point and further findings help to identify excited state tunnelling detachment (ESETD) after intersystem crossing (ISC), for further details see text. Modified from Ref. [131], Copyright 2021, Wiley-VCH.

orbitals - do overlap or at least relax differently according to their electronic environment. In this sense they are not at all isolated. In the absence of hybridization, unoccupied valence orbitals of the same orbital angular momentum – let us say empty *d* orbitals – complement the subshell and are thereby affected by the occupied orbitals. Therefore, vertical photo-excitations from the occupied inner $|p\rangle$ to the unoccupied valence $\langle d|$ orbitals (modulated by their overlap integral $\langle d|p\rangle$) probe not only the unoccupied valence orbitals but indirectly also the occupied valence orbitals. Due to conservation of orbital angular momentum – the $\Delta l = \pm 1$ selection rule – this scheme is very selective. The selectivity can be further increased by orienting the initial electronic moments in an applied external magnetic field and by fixing the sense of the photon spin by circular polarization. It was shown^[132] that in this case there will be a measurable X-ray induced magnetic circular dichroism (XMCD). Through sum rule analysis^[133,134] XMCD allows to determine the spin and orbital magnetic contributions to the total magnetic moments in coupled TM systems. After successful verification by application to solid state samples^[135,136] it took a while to recognize that this scheme may be transferred to the characterization of isolated samples as well, for example when held as cold ions within a magnetic ion trap and ionized/fragmented by absorption of circularly polarized X-ray radiation.^[137–139] Thereby, isolated iron, nickel and cobalt clusters have been characterized, and their cluster-size-dependent orbital angular momentum could be determined as induced by spin-orbit coupling.^[137–139]

In condensed phase, characterization of the magnetic anisotropies of ligand stabilized oligonuclear TM complexes is common and of great importance. The corresponding enthalpic difference of magnetization along so called “easy” and “hard” axes determines the persistence of induced magnetizations and thus the suitability of such “single molecule magnets” as single bits in data storage applications. The guinea pig of such endeavours is an acetate stabilized Mn_{12} complex^[140] that has been investigated extensively clearly showing considerable electronic coupling between the complex itself and the solid state support used to probe it. This raises the questions: how

large is the magnitude of the intrinsic magnetization and which of the Mn centers contribute to which extent? A recent gas phase XMCD^[141] study has now determined this intrinsic magnetization magnitude and compared it to bulk phase. In combination with high level “broken symmetry” density functional modelling^[142,143] it was found that the intrinsic magnetic texture of isolated Mn₁₂ complexes comes close to that of deposited complexes, excepting some reduction to Mn^{II} which can occur in the bulk as a result of radiation damage (cf. Figure 13). The high magnetization is thus an intrinsic feature of the Mn₁₂ coupled scaffold, that persists in spite of environmental influences but which can be influenced by reduction either at conductive surfaces or by radiation damage. The concomitant broken symmetry DFT modelling determines the easy axis’ of individual magnetic centers in Mn₁₂ acetate, and confirms robustness against ligand and geometry variations. The individual contributions to magnetization are found to be strong on the outer ring of eight Mn^{III}, and they are vanishingly small on the inner cubic core of four Mn^{IV}. Thus, the multi-method study achieves a high level of characterization of this prototypical magnetic TM complex and sets standards for subsequent studies dealing with magnetic textures of for example MnLnMn compounds,^[144] so called “ferric wheels”^[145] and other oligomeric TM compounds^[146] which are presently in the making.

Summary and Outlook

This review has focussed on advanced gas phase methods for in depth characterization of (primarily charged) oligonuclear TM compounds - presenting selected examples from the 3MET consortium to illustrate their application. Our review does not claim to cover bulk phase investigations of these or related

molecular systems but cites relevant studies if necessary. We have attempted to highlight the novel opportunities which arise not only for oligomeric TM compounds but also for other substance classes through the availability of the instrumentation alluded to. The corresponding methods range from high resolution electrospray ionization mass spectrometry (ESI-MS), which allows to characterize large fragile species by probing solution composition with little or no fragmentation upon volatilization. ESI-MS can also controllably generate isolated aggregates and counterion adducts thereof for collisional dissociation or laser spectroscopic studies. Other methods discussed include approaches for structurally probing electronic ground states, for example by means of ion mobility spectroscopy (IMS), infrared photon dissociation (IR-PD and IR-MPD) or corresponding double resonance techniques (2cIR-PD, IR-R2PI, etc.). Several of these methods also allow access to, discrimination of and/or interconversion between different isomers and conformers simultaneously present among the molecules probed. Isomer interconversion can be slowed and complex spectra simplified by vibrational cooling. Various ion trapping schemes have been developed to achieve the necessary cryogenization. This in turn allows for cryogenic messenger tagging which accesses one-photon dissociation (PD) measurements – both for electronic and vibrational spectroscopy of oligomeric TM compounds. We also briefly discuss time-resolved studies of ultrafast relaxation dynamics following electronic excitation of selected TM complexes - either by pump-probe PD in the case of cations or by pump-probe photoelectron spectroscopy (tr-PES) in the case of (multi)anions. A description of X-ray induced magnetic circular dichroism (XMCD) spectroscopy to study magnetic coupling in isolated multi TM complexes rounds off the discussion of electronic excitation methods.

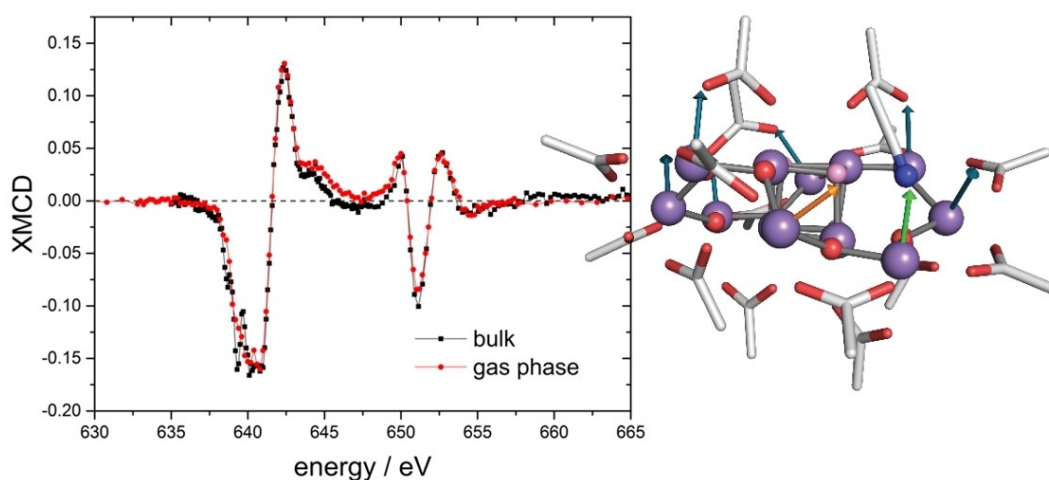


Figure 13. A synchrotron based gas phase ion trapping technique has been used to record XMCD spectra of oligonuclear TM complexes such as the Single Molecule Magnet (SMM) Mn₁₂ acetate in a cationic variant (left). The measurement proves that the intrinsic magnetic texture comes close to that of deposited complexes (apart from some reduction to Mn^{II} in the bulk as induced by radiation damage, evidenced by the minor deviation at 639 eV). Concomitant broken symmetry DFT modelling determines the easy axis’ of individual magnetic centers in Mn₁₂ acetate (right), the individual contributions found to be strong on the outer ring of eight Mn^{III} and vanishingly small on the inner cubic core of four Mn^{IV}. This study comprises a highlight of successful multi method characterization of isolated TM complexes as pioneered in 3MET. Reproduced with permission from Ref. [141], Copyright 2021, Wiley-VCH.

Just as in all modern synthetic efforts, application of the above mentioned experimental tools for the characterization of the ground and excited states of isolated oligomeric TM compounds requires description or verification by – and sometimes even confrontation with – state-of-the-art quantum chemical modelling. Consequently, the current review has also often mentioned the corresponding findings of quantum chemical approaches. It is however beyond the scope of this review to discuss the accuracies, computational expense and relative merits of those current quantum chemical methods available to model systems of interest to the 3MET consortium. We leave this task to a future endeavour.

We return to Scheme 1 of this review to finish with an outlook into the future. We believe that continued bidirectional feedback amongst all of three of the areas indicated, i.e. synthesis, spectroscopy and theory, will drive further progress in the field of multimetallic TM compounds and clusters. From our point of view it is now clear that advanced measurements on isolated 3MET systems such as those described here can aid both synthesis and theory – but much still needs to be done to advance the field via further gas-phase experimentation. For instance much of the established photophysics and photochemistry of applications-relevant members of the 3MET compound class such metalloporphyrin or metallophthalocyanine oligomers relies on condensed phase measurements which integrate over molecules in many different local redox environments (and thus different optical properties). Here, isomer-specific, inert-gas tagging probes of cryogenized samples will help to advance the corresponding quantum chemical descriptions by providing benchmark data. And there are more methods to come, such as for example the application of the Trapped Ion Electron Diffraction (TIED) technique which can provide for new, more direct insights into the structure (and thus TM-TM interactions) of TM cluster compounds and their corresponding aggregates.^[147] Also, interfacing gas-phase isomer and mass-selection technology with soft-landing deposition offers a new approach to understanding support interactions towards preparing novel devices based on TM compounds.

Acknowledgements

We thank the DFG for funding of the Collaborative Research Center, TRR 88 “3MET”. This has allowed the authors and their groups to collaborate over a timescale of more than ten years. MMK would also like to take the opportunity to thank past and present members of his group notably PD Dr. Patrick Weis, Dr. J.-G. Greisch, Erik Schneider, PD Dr. Oliver Hampe (deceased), Dr. Sergei Lebedkin and PD Dr. Detlef Schooss for interesting discussions and insights, several of which have found their way into this review. GNS acknowledges the many fruitful discussions with members of his group. He thanks the state research center OPTIMAS for long standing and ongoing support. Both authors also appreciate many constructive interactions with their 3MET colleagues. Open Access funding enabled and organized by Projekt DEAL.

Conflict of Interest

The authors declare no conflict of interest.

Keywords: cooperative effects · heterometallic complexes · spectroscopic methods

- [1] J. Chmela, M. E. Harding, D. Matioszek, C. E. Anson, F. Breher, W. Klopfer, *ChemPhysChem* **2016**, *17*, 37–45.
- [2] A. H. Jackson, G. W. Kenner, K. M. Smith, R. T. Aplin, H. Budzikiewicz, C. Djerassi, *Tetrahedron* **1965**, *21*, 2913–2924.
- [3] M. Yamashita, J. B. Fenn, *J. Chem. Phys.* **1984**, *88*, 4451–4459.
- [4] K. W. M. Siu, G. J. Gardner, S. S. Berman, *Org. Mass Spectrom.* **1989**, *24*, 931–942.
- [5] V. Katta, S. K. Chowdhury, B. T. Chait, *J. Am. Chem. Soc.* **1990**, *112*, 5348–5349.
- [6] A. van den Bergen, R. Colton, M. Percy, B. O. West, *Inorg. Chem.* **1993**, *32*, 3408–3411.
- [7] D. Dakternieks, H. Zhu, E. R. T. Tiekink, R. Colton, *J. Organomet. Chem.* **1994**, *476*, 33–40.
- [8] B. F. G. Johnson, S. McIndoe, *Coord. Chem. Rev.* **2000**, *200–202*, 901–932.
- [9] D. Fenske, T. Langetepe, M. M. Kappes, O. Hampe, P. Weis, *Angew. Chem. Int. Ed.* **2000**, *39*, 1857–1860; *Angew. Chem.* **2000**, *112*, 1925–1928.
- [10] N. G. Tsierkezos, J. Roithová, D. Schröder, M. Ončák, P. Slaviček, *Inorg. Chem.* **2009**, *48*, 6287–6296.
- [11] P. Weis, U. Schwarz, F. Hennrich, D. Wagner, S. Bräse, M. Kappes, *Phys. Chem. Chem. Phys.* **2014**, *16*, 6225–6232.
- [12] K. Müller, Y. Sun, A. Heimermann, F. Menges, G. Niedner-Schatteburg, C. van Wuelen, W. R. Thiel, *Chem. Eur. J.* **2013**, *19*, 7825–7834.
- [13] M. Gaffga, I. Munstein, P. Müller, J. Lang, W. R. Thiel, G. Niedner-Schatteburg, *J. Phys. Chem. A* **2015**, *119*, 12587–12598.
- [14] D. Hackenberger, B. Song, M. F. Grunberg, S. Farsadpour, F. Menges, H. Kelm, C. Gross, T. Wolff, G. Niedner-Schatteburg, W. R. Thiel, L. J. Goossen, *ChemCatChem* **2015**, *7*, 3579–3588.
- [15] F. Schon, M. Leist, A. Neuba, J. Lang, C. Braun, Y. Sun, G. Niedner-Schatteburg, S. Bräse, W. R. Thiel, *Chem. Commun.* **2017**, *53*, 12016–12019.
- [16] C. Groß, Y. Sun, T. Jost, T. Grimm, M. P. Klein, G. Niedner-Schatteburg, S. Becker, W. R. Thiel, *Chem. Commun.* **2020**, *56*, 368–371.
- [17] G. v. Helden, M. T. Hsu, P. R. Kemper, M. T. Bowers, *J. Chem. Phys.* **1991**, *95*, 3835–3837.
- [18] H. E. Revercomb, E. A. Mason, *Anal. Chem.* **1975**, *47*, 970–983.
- [19] D. E. Clemmer, R. R. Hudgins, M. F. Jarrold, *J. Am. Chem. Soc.* **1995**, *117*, 10141–10142.
- [20] P. Weis, S. Gilb, P. Gerhardt, M. M. Kappes, *Int. J. Mass Spectrom.* **2002**, *216*, 59–73.
- [21] J. C. May, J. A. McLean, *Anal. Chem.* **2015**, *87*, 1422–1436.
- [22] K. Giles, J. Ujma, J. Wildgoose, S. Pringle, K. Richardson, D. Langridge, M. Green, *Anal. Chem.* **2019**, *91*, 8564–8573.
- [23] C. Larriba-Andaluz, J. S. Prell, *Int. Rev. Phys. Chem.* **2020**, *39*, 569–623.
- [24] P. Weis, F. Hennrich, R. Fischer, E. K. Schneider, M. Neumaier, M. M. Kappes, *Phys. Chem. Chem. Phys.* **2019**, *21*, 18877–18892.
- [25] A. A. Shvartsburg, F. Li, K. Tang, R. D. Smith, *Anal. Chem.* **2006**, *78*, 3304–3315.
- [26] J. C. May, D. H. Russell, *J. Am. Soc. Mass Spectrom.* **2011**, *22*.
- [27] P. Weis, T. Bierweiler, E. Vollmer, M. M. Kappes, *J. Chem. Phys.* **2002**, *117*, 9293–9297.
- [28] R. Fromherz, G. Ganteför, A. A. Shvartsburg, *Phys. Rev. Lett.* **2002**, *89*, 083001.
- [29] F. Misaizu, N. Hori, H. Tanaka, K. Komatsu, A. Furuya, K. Ohno, *Eur. Phys. J. D* **2009**, *52*, 59–62.
- [30] P. Jäger, K. Brendle, E. Schneider, S. Kohaut, M. K. Armbruster, K. Fink, P. Weis, M. M. Kappes, *J. Phys. Chem. A* **2018**, *122*, 2974–2982.
- [31] K. Tang, A. A. Shvartsburg, H.-N. Lee, D. C. Prior, M. A. Buschbach, F. Li, A. V. Tolmachev, G. A. Anderson, R. D. Smith, *Anal. Chem.* **2005**, *77*, 3330–3339.
- [32] M. Vonderach, O. T. Ehrler, P. Weis, M. M. Kappes, *Anal. Chem.* **2011**, *83*, 1108–1115.
- [33] K. Brendle, U. Schwarz, P. Jäger, P. Weis, M. Kappes, *J. Phys. Chem. A* **2016**, *120*, 8716–8724.

- [34] G. Papadopoulos, A. Svendsen, O. V. Boyarkin, T. R. Rizzo, *Faraday Discuss.* **2011**, *150*, 243–255.
- [35] J. Seo, S. Warnke, K. Pagel, M. T. Bowers, G. von Helden, *Nat. Chem.* **2017**, *9*, 1263–1268.
- [36] A.-L. Simon, F. Chiro, C. M. Choi, C. Clavier, M. Barbaire, J. Maurelli, X. Dagany, L. MacAleese, P. Dugourd, *Rev. Sci. Instrum.* **2015**, *86*, 094101.
- [37] B. D. Adamson, N. J. A. Coughlan, P. B. Markworth, R. E. Continetti, E. J. Bieske, *Rev. Sci. Instrum.* **2014**, *85*, 123109.
- [38] P. Bansal, V. Yatsyna, A. H. Abikhodr, S. Warnke, A. Ben Faleh, N. Yalovenko, V. H. Wysocki, T. R. Rizzo, *Anal. Chem.* **2020**, *92*, 9079–9085.
- [39] M. T. Rodgers, K. M. Ervin, P. B. Armentrout, *J. Chem. Phys.* **1997**, *106*, 4499–4508.
- [40] J. Lang, M. Cayir, S. P. Walg, P. Di Martino-Fumo, W. R. Thiel, G. Niedner-Schatteburg, *Chem. Eur. J.* **2016**, *22*, 2345–2355.
- [41] J. Lang, J. M. Hewer, J. Meyer, J. Schuchmann, C. van Wüllen, G. Niedner-Schatteburg, *Phys. Chem. Chem. Phys.* **2018**, *20*, 16673–16685.
- [42] C. Kerner, J. Lang, M. Gaffga, F. S. Menges, Y. Sun, G. Niedner-Schatteburg, W. R. Thiel, *ChemPlusChem* **2017**, *82*, 212–224.
- [43] C. Kerner, J. P. Neu, M. Gaffga, J. Lang, B. Oelkers, Y. Sun, G. Niedner-Schatteburg, W. R. Thiel, *New J. Chem.* **2017**, *41*, 6995–7006.
- [44] K. Brendle, M. Kordel, E. Schneider, D. Wagner, S. Bräse, P. Weis, M. M. Kappes, *J. Am. Soc. Mass Spectrom.* **2018**, *29*, 382–392.
- [45] M. M. Kappes, R. H. Staley, *J. Am. Chem. Soc.* **1981**, *103*, 1286–1287.
- [46] K. Eller, H. Schwarz, *Chem. Rev.* **1991**, *91*, 1121–1177.
- [47] S. Peredkov, A. Savci, S. Peters, M. Neeb, W. Eberhardt, H. Kampschulte, J. Meyer, M. Tombers, B. Hofferberth, F. Menges, G. Niedner-Schatteburg, *J. Electron Spectrosc. Relat. Phenom.* **2011**, *184*, 113–118.
- [48] S. Dillinger, J. Mohrbach, J. Hewer, M. Gaffga, G. Niedner-Schatteburg, *Phys. Chem. Chem. Phys.* **2015**, *17*, 10358–10362.
- [49] S. Dillinger, G. Niedner-Schatteburg in *Cryo trapping by FT-MS for kinetics and spectroscopy*, **2019**, pp. 593–621.
- [50] D. Gerlich, S. Horning, *Chem. Rev.* **1992**, *92*, 1509–1539.
- [51] D. Gerlich, *J. Chem. Soc. Faraday Trans.* **1993**, *89*, 2199–2208.
- [52] D. Gerlich, *Phys. Scr.* **1995**, *1995*, 256–263.
- [53] P. B. Armentrout, J. L. Beauchamp, *Acc. Chem. Res.* **1989**, *22*, 315–321.
- [54] P. B. Armentrout in *Electronic state-specific transition metal ion chemistry*, Vol. 41 **1990**, pp. 313–344.
- [55] S. K. Loh, D. A. Hales, L. Lian, P. B. Armentrout, *J. Chem. Phys.* **1989**, *90*, 5466–5485.
- [56] P. B. Armentrout, *Science* **1991**, *251*, 175–179.
- [57] P. B. Armentrout in *Reactions and thermochemistry of small transition metal cluster ions*, *52* **2001**, pp. 423–461.
- [58] G. Niedner-Schatteburg in *Cooperative Effects in Clusters and Oligonuclear Complexes of Transition Metals in Isolation*, (Ed. S. Dehnen), Springer International Publishing, Cham, **2017**, pp. 1–40.
- [59] J. Hagen, L. D. Socaciu, M. Eljazyfer, U. Heiz, T. M. Bernhardt, L. Wöste, *Phys. Chem. Chem. Phys.* **2002**, *4*, 1707–1709.
- [60] L. D. Socaciu, J. Hagen, T. M. Bernhardt, L. Wöste, U. Heiz, H. Häkkinen, U. Landman, *J. Am. Chem. Soc.* **2003**, *125*, 10437–10445.
- [61] J. Hagen, L. D. Socaciu, J. Le Roux, D. Popolan, T. M. Bernhardt, L. Wöste, R. Mitrić, H. Noack, V. Bonacic-Koutecky, *J. Am. Chem. Soc.* **2004**, *126*, 3442–3443.
- [62] O. P. Balaj, I. Balteanu, T. T. J. Roßteuscher, M. K. Beyer, V. E. Bondybey, *Angew. Chem. Int. Ed.* **2004**, *43*, 6519–6522; *Angew. Chem.* **2004**, *116*, 6681–6684.
- [63] S. M. Lang, T. M. Bernhardt, R. N. Barnett, U. Landman, *Angew. Chem. Int. Ed.* **2010**, *49*, 980–983; *Angew. Chem.* **2010**, *122*, 993–996.
- [64] S. M. Lang, T. M. Bernhardt, *Phys. Chem. Chem. Phys.* **2012**, *14*, 9255–9269.
- [65] J. Roithova, D. Schröder, *Chem. Rev.* **2010**, *110*, 1170–1211.
- [66] J. Roithova, *Chem. Soc. Rev.* **2012**, *41*, 547–559.
- [67] J. Jašík, J. Zábka, J. Roithová, D. Gerlich, *Int. J. Mass Spectrom.* **2013**, *354–355*, 204–210.
- [68] J. Roithová, A. Gray, E. Andris, J. Jašík, D. Gerlich, *Acc. Chem. Res.* **2016**, *49*, 223–230.
- [69] N. Dietl, M. Schlangen, H. Schwarz, *Angew. Chem. Int. Ed.* **2012**, *51*, 5544–5555; *Angew. Chem.* **2012**, *124*, 5638–5650.
- [70] N. Dietl, C. Van Der Linde, M. Schlangen, M. K. Beyer, H. Schwarz, *Angew. Chem. Int. Ed.* **2011**, *50*, 4966–4969; *Angew. Chem.* **2011**, *123*, 5068–5072.
- [71] M. Schlangen, H. Schwarz, *Catal. Lett.* **2012**, *142*, 1265–1278.
- [72] C. Geng, J. Li, T. Weiske, M. Schlangen, S. Shaik, H. Schwarz, *J. Am. Chem. Soc.* **2017**, *139*, 1684–1689.
- [73] L.-X. Jiang, Q.-Y. Liu, X.-N. Li, S.-G. He, *J. Am. Soc. Mass Spectrom.* **2018**, *29*, 78–84.
- [74] W. Xue, Z. C. Wang, S. G. He, Y. Xie, E. R. Bernstein, *J. Am. Chem. Soc.* **2008**, *130*, 15879–15888.
- [75] X. L. Ding, X. N. Wu, Y. X. Zhao, S. G. He, *Acc. Chem. Res.* **2012**, *45*, 382–390.
- [76] Y. X. Zhao, X. G. Zhao, Y. Yang, M. Ruan, S. G. He, *J. Chem. Phys.* **2021**, *154*.
- [77] L. H. Mou, Y. Li, Z. Y. Li, Q. Y. Liu, Y. Ren, H. Chen, S. G. He, *J. Phys. Chem. Lett.* **2020**, *11*, 9990–9994.
- [78] G. D. Jiang, L. H. Mou, J. J. Chen, Z. Y. Li, S. G. He, *J. Phys. Chem. A* **2020**, *124*, 7749–7755.
- [79] Z. Y. Li, Z. Y. Li, Y. Li, Y. Li, Y. Li, L. H. Mou, L. H. Mou, L. H. Mou, J. J. Chen, J. J. Chen, J. J. Chen, Q. Y. Liu, Q. Y. Liu, S. G. He, S. G. He, S. G. He, H. Chen, H. Chen, *J. Am. Chem. Soc.* **2020**, *142*, 10747–10754.
- [80] L. H. Mou, G. D. Jiang, Z. Y. Li, S. G. He, *Chin. J. Chem. Phys.* **2020**, *33*, 507–520.
- [81] K. Lange, B. Visser, D. Neuwirth, J. F. Eckhard, U. Boesl, M. Tschurl, K. H. Bowen, U. Heiz, *Int. J. Mass Spectrom.* **2015**, *375*, 9–13.
- [82] M. Okumura, L. I. Yeh, J. D. Myers, Y. T. Lee, *J. Chem. Phys.* **1986**, *85*, 2328–2329.
- [83] J. H. Choi, K. T. Kuwata, B. M. Haas, Y. Cao, M. S. Johnson, M. Okumura, *J. Chem. Phys.* **1994**, *100*, 7153–7165.
- [84] T. Ebata, A. Fujii, N. Mikami, *Int. Rev. Phys. Chem.* **1998**, *17*, 331–361.
- [85] E. J. Bieske, O. Dopfer, *Chem. Rev.* **2000**, *100*, 3963–3998.
- [86] M. A. Duncan, *Int. Rev. Phys. Chem.* **2003**, *22*, 407–435.
- [87] J. M. Lisy, *J. Chem. Phys.* **2006**, *125*, 132302.
- [88] J. Roithová, *Chem. Soc. Rev.* **2012**, *41*, 547–559.
- [89] D. Guyer in *LaserVision*, Vol. **2010**, p. www.deanguyer.com.
- [90] P. Maitre, D. Scuderi, D. Corinti, B. Chiavarino, M. E. Crestoni, S. Fornarini, *Chem. Rev.* **2020**, *120*, 3261–3295.
- [91] J. Oomens, B. G. Sartakov, G. Meijer, G. von Helden, *Int. J. Mass Spectrom.* **2006**, *254*, 1–19.
- [92] W. Schöllkopf, S. Gewinner, H. Junkes, A. Paarmann, G. von Helden, H. Bluem, A. M. Todd, *The new IR and THz FEL facility at the Fritz Haber Institute in Berlin*, SPIE, **2015**, p.
- [93] B. M. Reinhard, A. Lagutschenkov, J. Lemaire, P. Maitre, P. Boissel, G. Niedner-Schatteburg, *J. Phys. Chem. A* **2004**, *108*, 3350–3355.
- [94] T. Pankewitz, A. Lagutschenkov, G. Niedner-Schatteburg, S. S. Xanthreas, Y. T. Lee, *J. Chem. Phys.* **2007**, *126*.
- [95] M. Okumura, L. I. Yeh, Y. T. Lee, *J. Chem. Phys.* **1985**, *83*, 3705–3706.
- [96] M. Okumura, L. I. Yeh, Y. T. Lee, *J. Chem. Phys.* **1988**, *88*, 79–91.
- [97] L. Jiang, T. Wende, R. Bergmann, G. Meijer, K. R. Asmis, *J. Am. Chem. Soc.* **2010**, *132*, 7398–7404.
- [98] M. Z. Kamrath, E. Garand, P. A. Jordan, C. M. Leavitt, A. B. Wolk, M. J. Van Stipdonk, S. J. Miller, M. A. Johnson, *J. Am. Chem. Soc.* **2011**, *133*, 6440–6448.
- [99] H. Schwarz, K. R. Asmis, *Chem. Eur. J.* **2019**, *25*, 2112–2126.
- [100] H. B. Oh, C. Lin, H. Y. Hwang, H. Zhai, K. Breuker, V. Zaboruski, B. K. Carpenter, F. W. McLafferty, *J. Am. Chem. Soc.* **2005**, *127*, 4076–4083.
- [101] J. C. Jiang, Y. S. Wang, H. C. Chang, S. H. Lin, Y. T. Lee, G. Niedner-Schatteburg, *J. Am. Chem. Soc.* **2000**, *122*, 1398–1410.
- [102] Y. Nosenko, C. Riehn, G. Niedner-Schatteburg, *Phys. Chem. Chem. Phys.* **2016**, *18*, 8491–8501.
- [103] N. I. Hammer, E. G. Diken, J. R. Roscioli, M. A. Johnson, E. M. Myshakin, K. D. Jordan, A. B. McCoy, X. Huang, J. M. Bowman, S. Carter, *J. Chem. Phys.* **2005**, *122*.
- [104] A. M. Ricks, A. D. Brathwaite, M. A. Duncan, *J. Phys. Chem. A* **2013**, *117*, 11490–11498.
- [105] J. Lang, M. Gaffga, F. Menges, G. Niedner-Schatteburg, *Phys. Chem. Chem. Phys.* **2014**, *16*, 17417–17421.
- [106] F. S. Menges, J. Lang, Y. Nosenko, C. Kerner, M. Gaffga, L. T. Ghoochany, W. R. Thiel, C. Riehn, G. Niedner-Schatteburg, *J. Phys. Chem. A* **2017**, *121*, 4422–4434.
- [107] J. M. Hewer, M. Lembach, Y. Nosenko, C. Riehn, G. Niedner-Schatteburg, *Int. J. Mol. Sci.* **2021**, submitted.
- [108] Y. Nosenko, F. Menges, C. Riehn, G. Niedner-Schatteburg, *Phys. Chem. Chem. Phys.* **2013**, *15*, 8171–8178.
- [109] B. Kwasiroch, J. Denton, E. Perez, T. Khuu, E. Schneider, A. Steiner, M. Theisen, S. Kruppa, P. Weis, M. Kappes, C. Riehn, M. Johnson, G. Niedner-Schatteburg, *Chem. Eur. J.* **2021**, to be published.
- [110] N. Heine, M. R. Fagiani, M. Rossi, T. Wende, G. Berden, V. Blum, K. R. Asmis, *J. Am. Chem. Soc.* **2013**, *135*, 8266–8273.
- [111] C. M. Leavitt, A. B. Wolk, J. A. Fournier, M. Z. Kamrath, E. Garand, M. J. Van Stipdonk, M. A. Johnson, *J. Phys. Chem. Lett.* **2012**, *3*, 1099–1105.

- [112] N. Yang, S. C. Edington, T. H. Choi, E. V. Henderson, J. P. Heindel, S. S. Xantheas, K. D. Jordan, M. A. Johnson, *Proc. Natl. Acad. Sci. USA* **2020**, *117*, 26047–26052.
- [113] N. Heine, K. R. Asmis, *Int. Rev. Phys. Chem.* **2015**, *34*, 1–34.
- [114] C. Geng, J. Li, T. Weiske, H. Schwarz, *Proc. Natl. Acad. Sci. USA* **2018**, *115*, 11680–11687.
- [115] C. Geng, J. Li, T. Weiske, H. Schwarz, *Proc. Natl. Acad. Sci. USA* **2019**, *116*, 21416–21420.
- [116] L.-H. Mou, Y. Li, Z.-Y. Li, Q.-Y. Liu, Y. Ren, H. Chen, S.-G. He, *J. Phys. Chem. Lett.* **2020**, *11*, 9990–9994.
- [117] D. V. Fries, M. P. Klein, A. Steiner, M. H. Prosenc, G. Niedner-Schatteburg, *Phys. Chem. Chem. Phys.* **2021**, *23*, 11345–11354.
- [118] J. Lang, J. Mohrbach, S. Dillinger, J. M. Hower, G. Niedner-Schatteburg, *Chem. Commun.* **2017**, *53*, 420–423.
- [119] J. Mohrbach, J. Lang, S. Dillinger, M. Prosenc, P. Braunstein, G. Niedner-Schatteburg, *J. Mol. Spectrosc.* **2017**, *332*, 103–108.
- [120] C. Riehn, C. Lahmann, B. Wassermann, B. Brutschy, *Chem. Phys. Lett.* **1992**, *197*, 443–450.
- [121] E. Gloaguen, M. Mons, K. Schwing, M. Gerhards, *Chem. Rev.* **2020**, *120*, 12490–12562.
- [122] M. D. Morse, *Acc. Chem. Res.* **2019**, *52*, 119–126.
- [123] S. V. Kruppa, F. Böppler, C. Holzer, W. Klopfer, R. Diller, C. Riehn, *J. Phys. Chem. Lett.* **2018**, *9*, 804–810.
- [124] A. H. Zewail, *J. Phys. Chem. A* **2000**, *104*, 5660–5694.
- [125] F. Liedy, F. Böppler, E. Waldt, Y. Nosenko, D. Imanbaev, A. Bhunia, M. Yadav, R. Diller, M. M. Kappes, P. W. Roesky, D. Schooss, C. Riehn, *ChemPhysChem* **2018**, *19*, 3050–3060.
- [126] M. Förstel, K. M. Pollow, K. Saroukh, E. A. Najib, R. Mitric, O. Dopfer, *Angew. Chem. Int. Ed.* **2020**, *59*, 21403–21408; *Angew. Chem.* **2020**, *132*, 21587–21592.
- [127] M. Förstel, O. Dopfer, *Chem. Eur. J.* **2021**, submitted.
- [128] J.-F. Greisch, M. E. Harding, B. Schäfer, M. Ruben, W. Klopfer, M. M. Kappes, D. Schooss, *J. Phys. Chem. Lett.* **2014**, *5*, 1727–1731.
- [129] X. B. Wang, H. K. Woo, X. Huang, M. M. Kappes, L. S. Wang, *Phys. Rev. Lett.* **2006**, *96*.
- [130] X. B. Wang, L. S. Wang in *Photoelectron spectroscopy of multiply charged anions*, Vol. 60, **2009**, pp. 105–126.
- [131] M.-O. Winghart, J.-P. Yang, M. Vonderach, A.-N. Unterreiner, D.-L. Huang, L.-S. Wang, S. Kruppa, C. Riehn, M. M. Kappes, *J. Chem. Phys.* **2016**, *144*, 054305.
- [132] G. van der Laan, B. T. Thole, *Phys. Rev. B* **1990**, *42*, 6670–6674.
- [133] B. T. Thole, P. Carra, F. Sette, G. Vanderlaan, *Phys. Rev. Lett.* **1992**, *68*, 1943–1946.
- [134] P. Carra, B. T. Thole, M. Altarelli, X. D. Wang, *Phys. Rev. Lett.* **1993**, *70*, 694–697.
- [135] C. T. Chen, Y. U. Idzerda, H. J. Lin, N. V. Smith, G. Meigs, E. Chaban, G. H. Ho, E. Pellegrin, F. Sette, *Phys. Rev. Lett.* **1995**, *75*, 152–155.
- [136] G. Schütz, E. Goering, H. Stoll in *Synchrotron Radiation Techniques Based on X-ray Magnetic Circular Dichroism*, **2007**.
- [137] S. Peredkov, M. Neeb, W. Eberhardt, J. Meyer, M. Tombers, H. Kampschulte, G. Niedner-Schatteburg, *Phys. Rev. Lett.* **2011**, *107*.
- [138] J. Meyer, M. Tombers, C. van Wüllen, G. Niedner-Schatteburg, S. Peredkov, W. Eberhardt, M. Neeb, S. Palutke, M. Martins, W. Wurth, *J. Chem. Phys.* **2015**, *143*.
- [139] A. Langenberg, K. Hirsch, A. Lawicki, V. Zamudio-Bayer, M. Niemeyer, P. Chmiela, B. Langbehn, A. Terasaki, B. V. Issendorff, J. T. Lau, *Phys. Rev. B* **2014**, *90*.
- [140] R. S. D. Gatteschi, J. Villain, *Molecular Nanomagnets*, Oxford University Press, Oxford, **2006**, p.
- [141] M. Tombers, J. Meyer, J. Meyer, A. Lawicki, V. Zamudio-Bayer, K. Hirsch, J. T. Lau, B. v. Issendorff, A. Terasaki, T. Schlathölder, R. Hoekstra, S. Schmidt, A. K. Powell, E. Kessler, M. H. Prosenc, C. v. Wüllen, G. Niedner-Schatteburg, *Chem. Eur. J.* **2021**, submitted 22.27.2021.
- [142] C. v. Wüllen, *J. Chem. Phys.* **2009**, *130*, 194109.
- [143] E. M. V. Kessler, S. Schmitt, C. van Wüllen, *J. Chem. Phys.* **2013**, *139*.
- [144] J. M. Hower, M. Tombers, J. Lang, S. Schmitt, Y. Lan, A. K. Powell, M. H. Prosenc, V. Zamudio-Bayer, J. T. Lau, B. von Issendorff, A. Terasaki, T. Schlathölder, R. Hoekstra, A. Bhunia, M. Yadav, R. Yadav, P. W. Roesky, G. Niedner-Schatteburg, **2021**, unpublished.
- [145] M. Tombers, J. Meyer, J. Hower, J. Meyer, A. Lawicki, V. Zamudio-Bayer, T. Lau, S. Schmidt, A. Powell, G. Niedner-Schatteburg, **2021**, unpublished.
- [146] M. Lembach, M. Luczak, Y. Mees, V. Zamudio-Bayer, M. Timm, M. Kubin, B. v. Issendorff, A. T., E. Brechin, J. T. Lau, G. Niedner-Schatteburg, **2021**, unpublished.
- [147] T. Rapps, R. Ahlrichs, E. Waldt, M. M. Kappes, D. Schooss, *Angew. Chem. Int. Ed.* **2013**, *52*, 6102–6105; *Angew. Chem.* **2013**, *125*, 6218–6221.

Manuscript received: August 2, 2021

Accepted manuscript online: October 11, 2021

Version of record online: October 27, 2021